

Heavy Metals Distribution in Mangrove Leaves in Various Sudanese Coastal Zones at The Red Sea

Rabha Khalil Mohammad Khalil¹, Kashif Ali Solangi^{2,3*}, Abdullahi Bala Alhassan⁴, Waseem Razzaq Khan⁵ and Mohammed Othman Aljahdali^{6*}

¹Department of Marine Biology Faculty of Marine Sciences & Fisheries, Red Sea University, Portsudan, Sudan.

² School of Tropical Agriculture and Forestry, Hainan University, China.

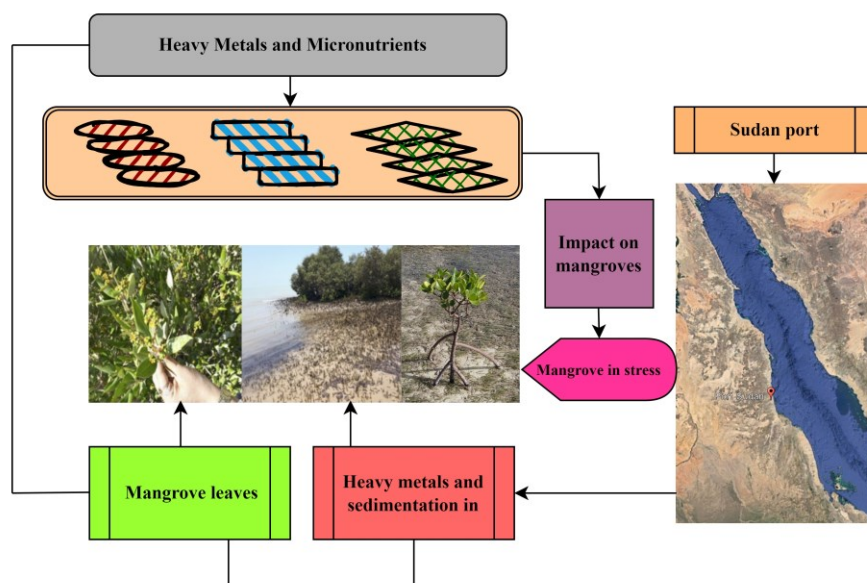
³Key Laboratory of Genetics and Germplasm Innovation of Tropical Special Forest Trees and Ornamental Plants (Ministry of Education), School of Tropical Agriculture and Forestry, Hainan University.

⁴Department of Biology, Faculty of Life Sciences, Ahmadu Bello University, Zaria 810001, Nigeria

⁵Department of Forestry Science and Biodiversity, Faculty of Forestry and Environment, Universiti Putra Malaysia, 43400 Serdang, Malaysia

⁶Department of Biological Sciences, Faculty of Science, King Abdulaziz University, Jeddah 21589, Saudi Arabia

*Correspondence: 5103180312@stmail.ujs.edu.cn: moaljahdali@kau.edu.sa



Graphical Abstract

ABSTRACT

Mangrove ecosystem contamination, especially in the Red Sea region, has caused major concerns on a worldwide scale. The heavy metal accumulation typical of a mangrove species, *Avicenna marina* L., (*A. marina*) leaves and soluble salts in sediments have not been studied on the Red Sea coast of Sudan. The present study investigates the two nutrients calcium (Ca) and iron (Fe) and heavy metals such as barium (Ba), titanium (Ti), and strontium (Sr) in the mangrove species *A. marina* in the leaves of six different locations in the Red Sea coastal area, as follows: (Hamasyat (HM) Keligo (KG), and Enkfel (EK) of the Gulf of Dunnabeb, and three sites were selected in the south of the Sudanese coast as follows: (Amarat Island (AM), Ibn Abbas Island (BN), and Ras Kassar (RK)). The results demonstrate that the maximum calcium (Ca) and iron (Fe) concentrations in mangrove leaves were 35.9 mg/kg and 4.10 mg/kg recorded at RK and AM, respectively, in the south region of the Red Sea. The heavy metal concentrations (mg/kg) vary between different locations. The higher concentration of heavy metals in mangrove leaves increased as Ba was 1.1 mg/kg in the EG north region. While Ti (0.5 mg/kg) and Sr (2.80 mg/kg) higher concentrations were recorded in AM and EK, respectively, in the south area than in the other experimental sites. Heavy metals and soluble salts in sediments are continuously monitored in mangrove habitats to ensure they keep within allowed limits. These

34 results could be useful as a database for prospective ecological research, preservation efforts, and long-term
35 sustainable management of the Sudanese mangrove ecosystems throughout the Red Sea coastal.

36 **Keywords:** heavy metal contamination, *Avicennia marina*, soluble salts, Red Sea

37 **1. Introduction**

38 Mangrove plant species play a crucial role in maintaining the health and stability of coastal
39 ecosystems (Saoum and Sarkar, 2024). These plants are mostly found between the land and sea
40 areas flooded with tidal waters, mainly at upper water levels and subject to storms in tropical and
41 semi-tropical regions (Aljahdali and Alhassan, 2020). The fast growth of the marine sector and a
42 major change in the world climate are attracting the ecological significance of mangroves to the
43 attention of many people, making their protection a global concern (Ali Solangi et al., 2022).
44 However, mangrove plays a major role in the fight against global warming, coastal erosion, and
45 the storage of enormous quantities of carbon in sediments as a natural barrier (Anu et al., 2024).
46 Heavy metal pollution is a key environmental dilemma as the metals in contaminated sediments
47 may gather in the various organisms of the estuarine ecosystem and ultimately enter the food chain,
48 thereby affecting the human (Afzaal et al., 2022). There are several studies that cultivated
49 mangrove species as dependable bio-indicators for heavy metal contamination (Ashournejad et al.,
50 2019; Jimenez et al., 2021). Due to the metal toxicity and bioaccumulation potential determination,
51 the cycling of heavy metals is a serious concern in mangrove environments (Wang et al., 2024).
52 Heavy metals, which cannot degrade, would accumulate in plant tissues after being transported
53 from soils, where they would cause adverse effects on plants. Mangrove trees can store metals,
54 transferring these elements from the sediment and concentrating them in their tissues (Nguyen et
55 al., 2020). Mangroves remove heavy metals through chemical processes: absorption, cation
56 exchange, and filtration, through their various mechanisms (Dubey et al., 2018). A research study
57 main focused on a higher range of heavy metals in leaf matter for several mangrove species, such
58 as true mangrove and white mangrove (Badarudeen et al., 2014). This attribute makes *Avicennia*
59 *marina* L (*A. marina*) a valuable species, allowing scientists to use experimental testing and
60 monitoring to gather quantitative data regarding the environmental health of its habitat
61 (Einollahipeer et al., 2013). The ability of mangrove species to resist removal, control heavy metal
62 uptake at the roots, and limit their movement to the shoots (Arumugam et al., 2018). Mangrove
63 performs an important role in coastal areas; they provide shelter; they grow in abundance in saline
64 soil and salty water, frequently inundated with fresh and saltwater (Kamaruzzaman et al., 2009).
65 Previously, some studies focus on mangrove mapping through different satellite images and state

66 that 75% using NDVI (Normalized Difference Vegetation Index) (Aslam et al., 2023), machine
67 learning method (Aslam et al., 2024a) and land use land cover technique (Aslam et al., 2024b). A
68 research study reported that mangrove biomass also determine with remote sensing technique but
69 also need some validation points with field data (K. A. Solangi et al., 2019). Therefore, field data
70 very important a research revealed that many mangrove species in the field accumulate metals,
71 including copper (Cu), zinc (Zn), lead (Pb), iron (Fe), manganese (Mn), and cadmium (Cd), mostly
72 in their roots and leaves (Khan and Aljahdali, 2022).

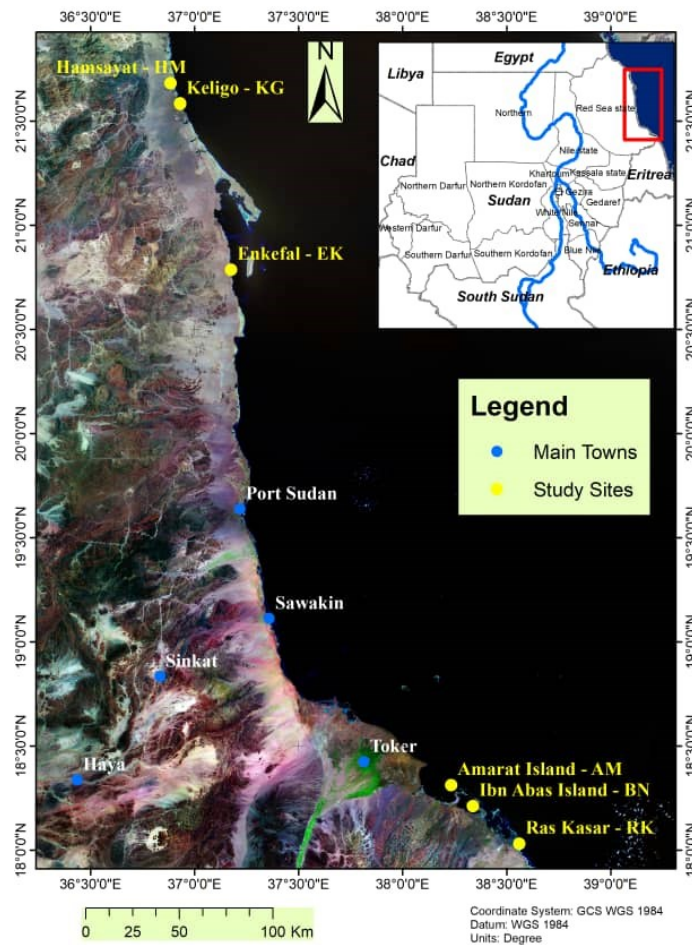
73 Some studies suggested that mangroves may accumulate and translocate some metals with leaf
74 Bioconcentration Factors (BCFs) greater than one, e.g. 1.5–2.4 for *A. marina* 1.7 for *Aegiceras*
75 *corniculatum* and 1.2 for *Kandelia candel* (Chen et al., 2013). In this context, mangrove *Avicennia*
76 *marina* grows in the intertidal zones along the eastern coastlines of the Arabian Peninsula, forming
77 discrete communities in several locations (Abou Seedo et al., 2017). These complex root systems,
78 like those of other coastal species, can help slow the erosion rate by promoting sediment
79 development within their complex structures. Various species of mangroves have a unique capacity
80 to develop and adapt to their surroundings, enhancing coastlines with their intricate root systems
81 and promoting plant growth (Solangi et al., 2021). The mangrove ecosystem in Bahrain becomes
82 polluted in many ways, most notably by wastewater discharge from the Tubli sewage treatment
83 plant and, to some extent, by urban and industrial runoff. This study investigates the heavy metals
84 distribution in the mangrove leaves as affected by the urban community wastewater release in three
85 mangrove places in the Tubli Bay area (Bartolini et al., 2011). Nazli and Hashim (2010) reported
86 Cu and Pb concentrations in the roots and leaves of crabapple mangroves. They concluded that the
87 roots of this species had a high capacity to take up heavy metals and could be a viable
88 phytoremediation species for heavy metal treatment in Malaysian mangrove ecosystems. A
89 previous study examined the effects of heavy metals inflowing into the estuaries and the overall
90 health of the mangrove ecosystem in a coastal area of south Gujarat, India (Dudani et al., 2017).
91 An earlier research was carried out in the region (Rabigh lagoon) in Saudi Arabia; the primary
92 purpose of this research was to examine the physiological response to heavy metals in *A. marina*
93 leaves and to assess ecological risk by determining the concentrations of these metals in coastal
94 sediment (Aljahdali and Alhassan, 2020). One of the world's most at-risk areas for rising sea
95 levels, both in terms of the area of low-lying land inundated and the percentage of populations
96 influenced, is the Mekong River Delta (MRD) in Vietnam, which is inhabited by enormous and

97 ever-changing mangrove forests (Dasgupta, 2007). Using a dataset of published research from the
98 literature, metal concentrations were measured in mangrove sediments and mangrove root and leaf
99 tissue in different countries. Keeping this view, present study focuses on heavy metals
100 contamination in the mangrove environments in Sudan. Mangrove forests most of the vegetation
101 on the Red Sea coast of Sudan and are subject by *A. marina*. Particular, the mangrove ecosystems
102 have not received enough attention in relation to this research. The main objective of the present
103 to find out the status of three heavy metals such as barium (Ba), titanium (Ti), and strontium (Sr)
104 and two nutrients calcium (Ca) and iron (Fe) in the leaves of mangrove species (*Avicennia*
105 *marina*.L.) at the six different locations of Red Sea coastal. The distribution pattern of certain
106 heavy metals in mangrove leaves is investigated in order to understand the essential role of
107 mangrove plants in the cycling of these metals.

108 **2. Material and method**

109 *2.1 Study Area*

110 The study was conducted in six regions, three areas selected in north of the Sudanese coast as
111 follows: (Hamasyat (HM), Keligo (KG)- Enkfel (EK) of the Gulf of Dungenab and three sites
112 were selected in south of the Sudanese coast as follows: (Amarat Island (AM), Ibn Abbas Island
113 (BN) and Ras Kassar (RK)) of the Aqib region with the coordinates of 20° 16' 48.835" N and 38°
114 30' 45.263 E (figure. 1) to investigate the mangrove species *A. marina*. The area is characterized
115 by a semi-arid climate with a mean daily temperature of 29 °C in winter and 42°C in summer.
116 Annual rainfall averaged 164 mm, tides are unusual, with a mean spring tide of 0.1 m.



117
 118 **Figure 1.** Location map of six different sites of study area.

119 *2.2 Soil sampling*

120 Soil samples were randomly collected from six different locations in the Red Sea coastal area of
 121 Sudan in the winter season from December 2022 to February 2023. The coordinates were recorded
 122 using a hand-held Garmin GPS-62s device. Prior to the field survey, sampling points were inputted
 123 into the GPS-62s to facilitate route tracking and identify convenient sampling locations. Soil
 124 samples were collected with a soil auger, packed into plastic bags, labelled with the sampling
 125 location, and carried to the Sudan University of Science and Technology, Soil Department
 126 laboratory for the physio-chemical analysis. The samples were air-dried at room temperature and
 127 sifted through 2-mm and < 2-mm sieves. For the electrical conductivity (EC) analysis, the < 2-mm
 128 fraction was utilized. Subsample portions were set aside for soil pH and nutrient analysis. Total 55
 129 soil samples were collected from various locations within the selected areas. A subsample portion

130 of a 2-mm mesh after oven drying (40 °C) for 48 h was also used for soil textural class
131 measurements. Soil textural classes, sediments particles size distribution and its percentages were
132 estimated by the field texture determination method (FAO, 2006).

133 *2.3 Plant sample preparation*

134 Mangrove leaves were plucked in different locations to analyse nutrients and heavy metals.
135 Samples were analysed using an XRF device in atomic energy, Khartoum. First, samples were
136 washed with distilled water to remove any sand and debris, then air-dried for seven days. The dried
137 sample was crushed and kept in airtight cellophane until it was time to utilize it. To obtain a
138 noticeable and comprehensive extraction of the active components in the plant samples, about 10
139 g of the mangroves. 1.0 g of the powdered sample was pressed by (15 tons per cm. For quality
140 control, four standard reference materials were used and treated in the same manner.

141 *2.4 XRF measurement*

142 Dispersive energy XRF spectroscopy with a resolution of 109 keV using an ORTKC Si (Li)
143 detector. The major source employed to measure Ca, Cr, Cu, Fe, K, Mn, Ni, Sr, and Zn in some
144 wild edible plants from Sudan was radioisotope Cd, which has an energy of 22.1 KeV. The XRF
145 spectrometer was used to measure plant pellets, and each measurement took three thousand
146 seconds. A Cd-109 x-ray source was used to excite x-rays, and the resulting spectra were then
147 uploaded to a computer. After that, the spectra were examined, and the computer's AXIL-XRF
148 program was used to determine the elements' concentration in the samples. For quality control,
149 hay powder was used as a standard reference and handled identically. A standard reference of hay
150 powder was used for quality control (Ebrahim et al., 2012).

151 For RBS studies, backscattered particles of a 3 MeV proton beam at a scattering angle θ of 165°
152 were found using a silicon PIPS detector from Canberra with 14 keV of energy resolution and
153 25mm of active area. The experimental setup has been described in detail elsewhere. (Roumié et
154 al., 2004). Analyses have become powerful analytical methods for multi-element analysis (Ahmed,
155 2014). The characteristic X-rays that are emitted are measured by a high-resolution X-ray detector
156 (liquid nitrogen-cooled Si or Li). Twenty to twenty-five elements can be found at the same time
157 using the XRF multi-element analysis technology (Markowitz *et al.*, 2002). Benefits include little
158 sample preparation, non-destructiveness, use across a broad range of concentrations, good
159 precision and accuracy, and the ability to assess solid, powder, and liquid samples. It is also almost
160 independent of the chemical state of the fee-based analyte. Certain drawbacks, like x-rays. The fee

161 sample has limited penetration (1 mm layer), and light elements (below Na) have extremely low
162 sensitivity. However, although is feasible on a novel instrument, limits of detection are only
163 moderate, inter-element (MATRIX) effects could be significant and necessitate computer
164 correction, and instrumentation is relatively expensive (Clapera, 2006).

165 *2.5 Organic matter*

166 Removal of small amounts of organic matter (organic carbon less than 05%) is unnecessary. When
167 HCL is used, subsequent treatments will remove soluble salts and iron oxides and aluminum. Salt
168 washing will reduce gypsum, if present to an amount that will not interfere with the proper
169 dispersion of soil particles. FAO Soil Bulletin 10 (1984) J. Dewis and F. Feitas Harmful effect of
170 CaCO_3 . (1) Fixation of phosphate (po_4)³ (2) unavailability of iron; oxides ferrous into ferrous (3)
171 loss of ammonia: CaCO_3 increases pH and produces OH while reacting with NH_4 .

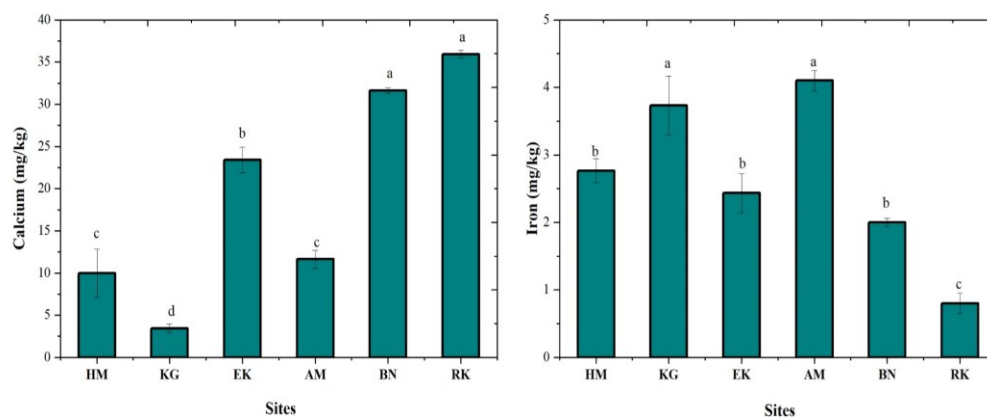
172 *2.5 Data analysis*

173 One-way ANOVA was used to determine significant changes in heavy metal concentrations in *A.*
174 *marina* leaves and soluble salts in sediment. Where there significant difference, Duncan's Multiple
175 Range tests at a significant level of $P < 0.05$ was used to separate the mean values. IBM SPSS
176 Statistics version 20.0 (Corp., Armonk, NY, USA) was used for the analysis. Origin Pro 9.0
177 (Northampton, Massachusetts, USA) was used to create the Calcium (Ca), Magnesium (Mg) and
178 Nitrogen (N), frequency (%) and soil sediments frequency (%) graphs.

179 **3. Results**

180 *3.1 Potassium and iron concentration in mangrove leaves*

181 The amounts of calcium (Ca) and iron (Fe) in mangrove species (*A. marina* leaves were different
182 in various regions of the Red Sea coast in Sudan, in the north (HM, KG, and EK) and the south
183 (AM, BN, and RK) figure 2. The maximum Ca concentration in mangrove leaves was observed at
184 two south locations of the red sea coast, by RK and BN, at 35.9 mg/kg and 31.6 mg/kg. However,
185 a minimum Ca concentration in mangrove leaves was noted in the north area of Red Sea KG by
186 3.4 mg/kg. The greater Fe concentration in mangrove leaves was recorded in the south region of
187 the Red Sea AM by 4.10 mg/kg compared to the entire experimental location. While the lowest Fe
188 (0.80 mg/kg) concentration was also noted in the south region compared to the north regions of
189 the Red Sea, these findings suggest that soil type and mangrove development affect the
190 concentration of Ca and Fe across sites.



191
 192 **Figure 2.** Determination of calcium (Ca) and iron (Fe) absorption concentrations in mangrove
 193 species at six various north and south Red Sea coastal regions. Based on Duncan's multiple tests,
 194 The letters specify significant influences at $p < 0.05$, replicates $n = 3$.
 195 *Note:* North regions: Hamasyat (HM), Kelijo (KG), Enkfel (EK), and South regions: Amarat Island
 196 (AM), Ibn Abbas Island (BN), and Ras Kassar (RK) of Red Sea coast in Sudan.

197 3.2 Examination of heavy metals in mangrove leaves

198 The heavy metal concentrations such as barium (Ba), titanium (Ti), and strontium (Sr) in the
 199 mangrove species (*A.marina*. presented a huge amount of difference in the mean concentrations
 200 collected from the Red Sea coast in Sudan. The heavy metal range in the mangrove leaves at each
 201 site is shown in table 1. The results for Ba indicate non-significant differences across six different
 202 areas, while Ba was found to have a higher value, i.e., 1.1 mg/kg, in EG on the north side of the
 203 Red Sea coast. In contrast, significant ($p < 0.05$) differences were observed for the Ti and Sr mg/kg
 204 heavy metal concentrations. Specifically, higher concentrations of Ti by 0.5 mg/kg were observed
 205 in the AM south region. Whereas maximum concentrations of Sr by 2.80 mg/kg were observed at
 206 the south location of the EK site compared to other areas.

207
 208 **Table 1.** Heavy metals Barium (Ba), Titanium (Ti) and Strontium (Sr) mg/kg concentrations in
 209 mangrove species (*A.marina* at six various north and south red sea coastal regions. The different
 210 letters specify significant influences at $p < 0.05$, replicates $n = 3$, based on Duncan's

Sites	Ba (mg/kg)	Ti (mg/kg)	Sr (mg/kg)
HM	0.3±0.06 ^a	0.2±0.05 ^{bc}	0.16±0.03 ^b

KG	0.2±0.03 ^a	0.4±0.05 ^{ab}	0.13±0.03 ^b
EK	1.1±0.09 ^a	0.1±0.01 ^c	2.80±1.20 ^a
AM	0.2±0.02 ^a	0.5±0.12 ^a	0.13±0.02 ^b
BN	0.2±0.05 ^a	0.1±0.03 ^c	0.36±0.03 ^b
RK	0.2±0.03 ^a	0.2±0.05 ^{bc}	0.50±0.02 ^b

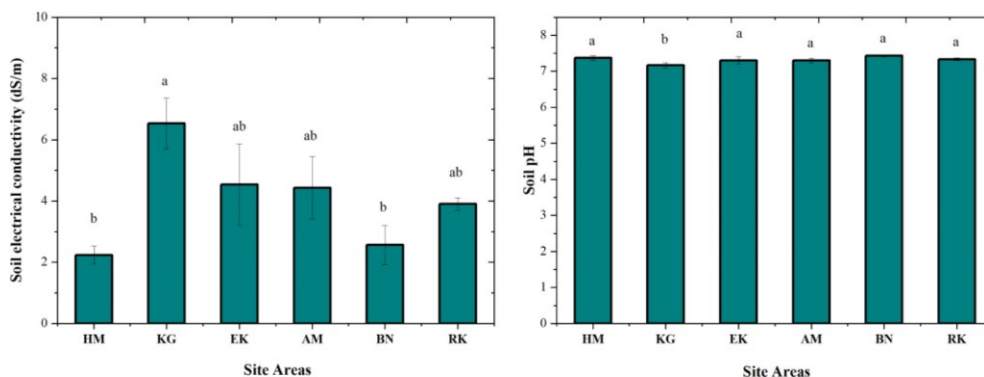
211 multiple tests.

212

213 *Note:* North regions: Hamasyat (HM), Kelijo (KG), Enkfel (EK), and South regions: Amarat Island
214 (AM), Ibn Abbas Island (BN), and Ras Kassar (RK) of Red Sea coast in Sudan.

215 3.3 Electrical conductivity (EC) and soil pH (pH)

216 The presented data on electrical conductivity (EC) and soil pH showed variance for different
217 locations of Red Sea coastal areas shown figure 3. However, soil EC showed changes across the
218 entire experimental location. At the same time, the highest EC value was noted at 6.5 dS/m in KG
219 on the north side of the study area, while the lowest EC level was recorded at 2.2 dS/m in HM in
220 the north area of the Red Sea. The greater soil pH was observed in the BN south region, and the
221 lowest soil pH was recorded at 7.1 on the KG north side of the experimental sites.



222

223 **Figure 3.** The figure shows ranges of EC and pH under cultivation mangrove (*A. marina*) at six
224 various north and south Red Sea coastal regions. Based on Duncan's multiple tests, The letters
225 specify significant influences at $p < 0.05$, replicates $n = 3$.

226 *Note:* North regions: Hamasyat (HM), Kelijo (KG), Enkfel (EK), and South regions: Amarat Island
227 (AM), Ibn Abbas Island (BN), and Ras Kassar (RK) of Red Sea coast in Sudan.

228

229 3.4 Soluble salt concentration in sediments

230 The concentrations of soluble saltssodium (Na), chloride (Cl), bicarbonate (HCO₃), and carbon
 231 trioxide (CO₃), for the different experimental areas are described in table 2. Different salt ranges
 232 vary in different regions of the Red Sea area. The higher Na and Cl concentration ranges were 56.3
 233 meq/L⁻¹ and 49.1 meq/L⁻¹, respectively, presented in KG, the north area of the Red Sea. Similarly,
 234 lower salt concentrations were recorded in the HM north side of the coastal area. Therefore, the
 235 maximum concentration of HCO₃ salt was 14.5 meq/L on the EK north side of the study area.
 236 While the lowest concentration of HCO₃ was found in the BN region, which was 6.8 meq/L⁻¹ across
 237 all locations. The greater range of CO₃ was 3.62 meq/L⁻¹, recorded in the north area of the study,
 238 and the lowest value was also recorded in the north side of the study location. Most of the soluble
 239 salt concentrations were recorded in the northern region of the Red Sea coastal area.

240 **Table 2.** Chlorine (CL), Hydrogen carbonate (HCO₃), Carbon trioxide (CO₃) and sodium (Na) of
 241 six different locations.

Study Site	Na (meq/L ⁻¹)	CL (meq/L ⁻¹)	HCO ₃ (meq/L ⁻¹)	CO ₃ (meq/L ⁻¹)
HM	9.3±1.45 ^c	14.3±2.3 ^c	8.8±0.6 ^c	1.33±0.31 ^c
KG	56.3±4.25 ^a	49.1±7.4 ^a	16.3±1.0 ^a	3.62±0.32 ^a
EK	34.8±8.91 ^b	31.1±9.9 ^{abc}	14.5±0.2 ^{ab}	3.33±0.33 ^a
AM	37.6±8.8 ^{ab}	36.1±7.1 ^{bc}	10.8±2.9 ^a	2.66±0.28 ^{ab}
BN	20.1±5.50 ^{bc}	18.0±4.5 ^{bc}	6.8±2.1 ^c	1.66±0.26 ^{bc}
RK	31.6±2.60 ^b	27.1±2.1 ^{bc}	9.6±0.33 ^c	2.66±0.22 ^{ab}

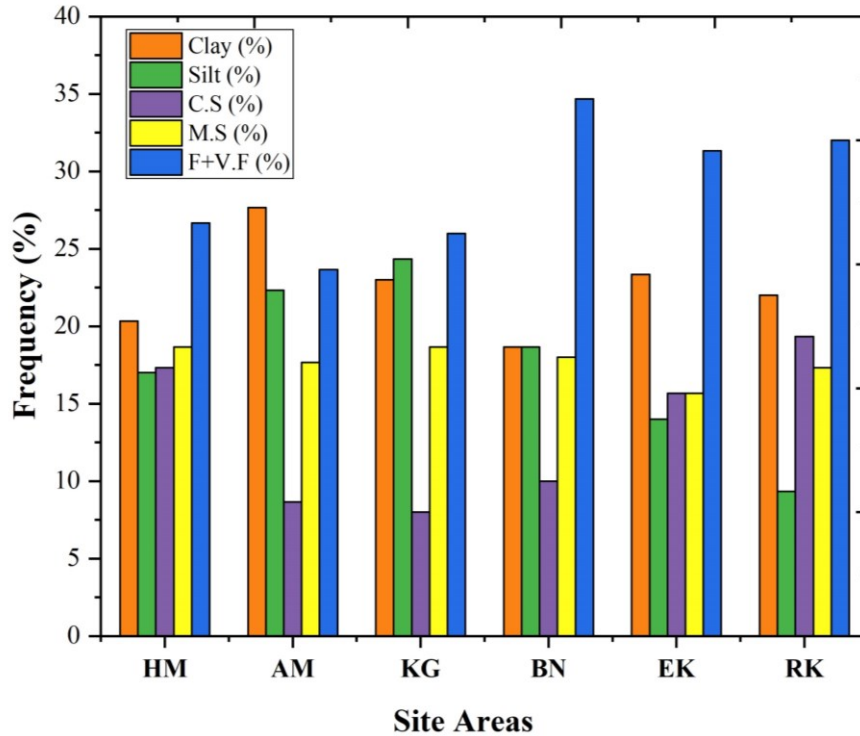
242

243 3.5 Soil sediment frequency percentages

244 The frequency percentages of the size of sediment particles (e.g., clay, silt, carafe sand, medium
 245 sand, fine sand, and very fine sand) showed changes across the various experimental sites (figure
 246 4). However, figure 3 showed that fine and very fine sand particles were dominant mostly in the
 247 south area of the study region. The highest frequency percentages were found in the BN site, at
 248 34.7%, for fine and very fine sand particles. The highest clay frequency was 27.7% recorded in
 249 AM in the south region. Among all sediment particles, carafe sand showed lower frequency
 250 percentages in AM, KG, BN, and EK: 8.6%, 8.0%, 10.0%, and 15.6%, respectively.

251

252

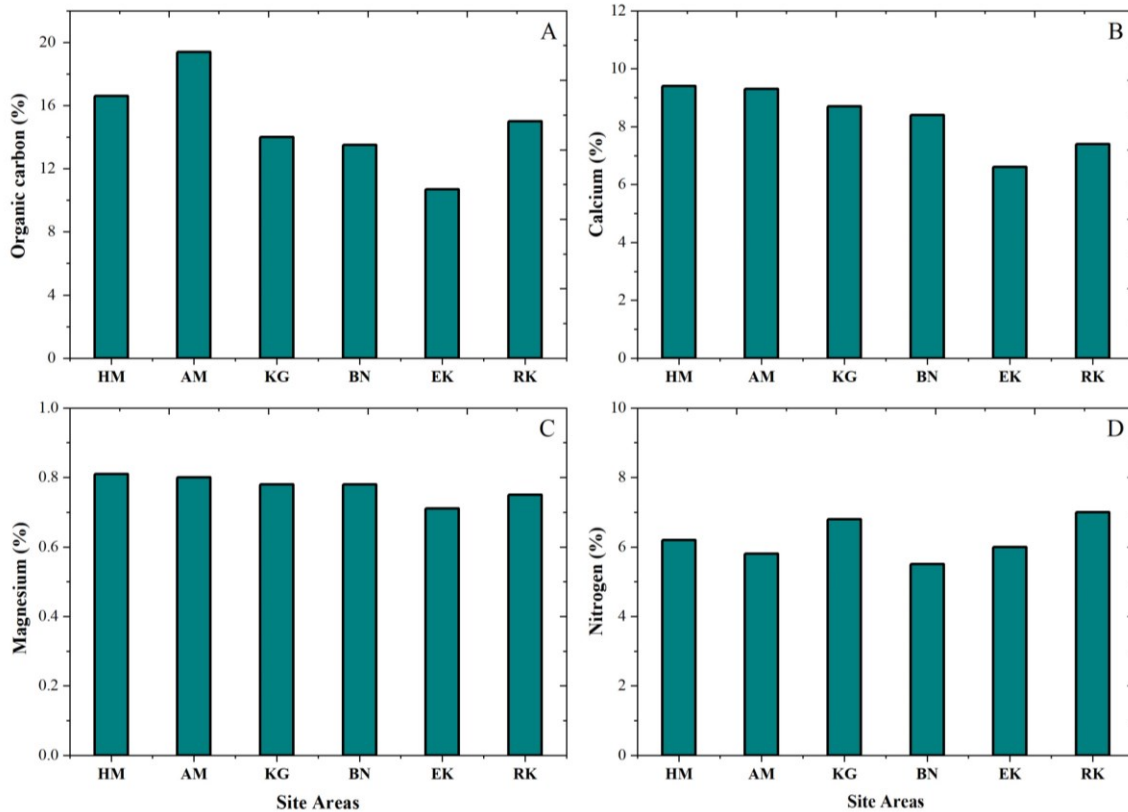


253

254 **Figure 4.** This figure shows soil textural classes of six different coastal areas' north and south
 255 locations. North regions: Hamasyat (HM), Kelijo (KG), Enkfel (EK), and South regions: Amarat
 256 Island (AM), Ibn Abbas Island (BN), and Ras Kassar (RK) of the Red Sea coast in Sudan
 257 *Note:* CS: (Carafe sand), MS: (medium sand), and F+VF: (fine sand and very fine sand)

258 3.6 Nutrient percentages in sediments

259 Sediment nutrient percentages, organic carbon (OC), calcium (Ca), magnesium (Mg), and nitrogen
 260 (N), presented the modification among all study locations figure 5. The highest OC was 19.4%
 261 found in AM in the north area. The lowest OC was 10.7% in EK in the south region, and higher Ca
 262 percentages in sediments were observed in the following directions: 9.4%, 9.3%, and 8.7%, i.e.,
 263 HM, AM, and KG, respectively, in the north region. Meanwhile, Mg percentages also increased
 264 on the north side of the Red Sea coastal area. The highest N in sediment was 7% observed in RK
 265 in the southern regions. The lowest N in sediments was 5%, which was noted in BN in the north
 266 region and RK in the south region of the Red Sea coast in Sudan.



267

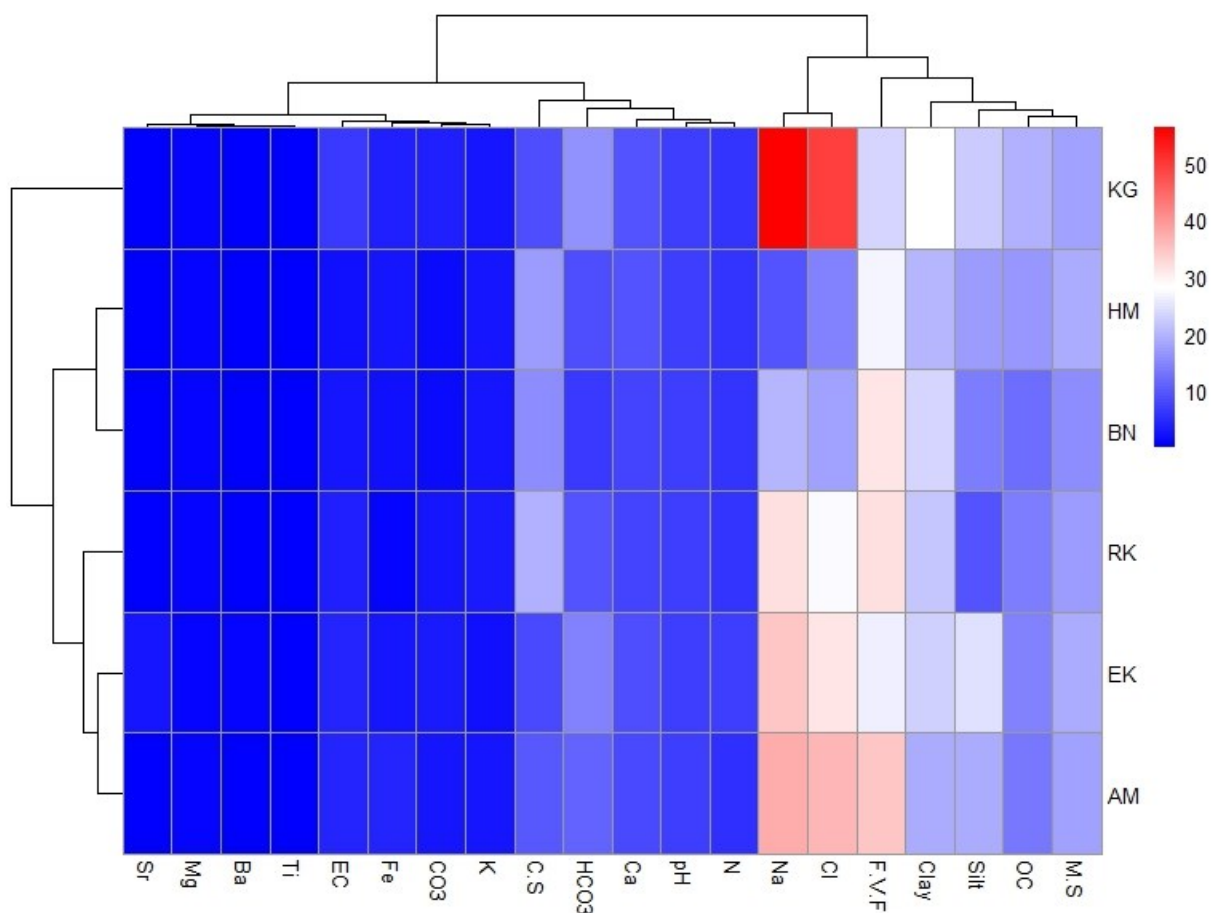
268

269 **Figure 5.** This figure shows the nutrient percentages of organic carbon (OC), n calcium (Ca),
 270 magnesium (Mg), and nitrogen (N) in the sediments of six different north and south locations of
 271 coastal areas. North regions: Hamasyat (HM), Kelijo (KG), Enkfel (EK), and South regions:
 272 Amarat Island (AM), Ibn Abbas Island (BN), and Ras Kassar (RK) of the Red Sea coast in Sudan

273 *3.7 Influence of Sediment Grain Sizes on Heavy Metals and Nutrients*

274 The cluster heat map revealed the relationship between the sites and other dependent variables
 275 such as the heavy metals, nutrients and soil grain sizes (figure 5). The cluster for the six sites, at
 276 the highest similarity level, revealed a close relationship between the sites except for site KG.
 277 Additionally, Na and Cl showed more association with site KG. Two groups were formed for the
 278 independent variables at the highest similarity level. Na, Cl, F+V.F, clay, silt, OC and M.S form a
 279 single group, revealing that Na, Cl, OC and M.S. were more associated with clay and silt grain
 280 types. However, the second group was formed containing Sr, Mg, Ti, EC, Fe, CO₃, K, C.S. HCO₃,
 281 Ca, pH and N (figure 6).

282



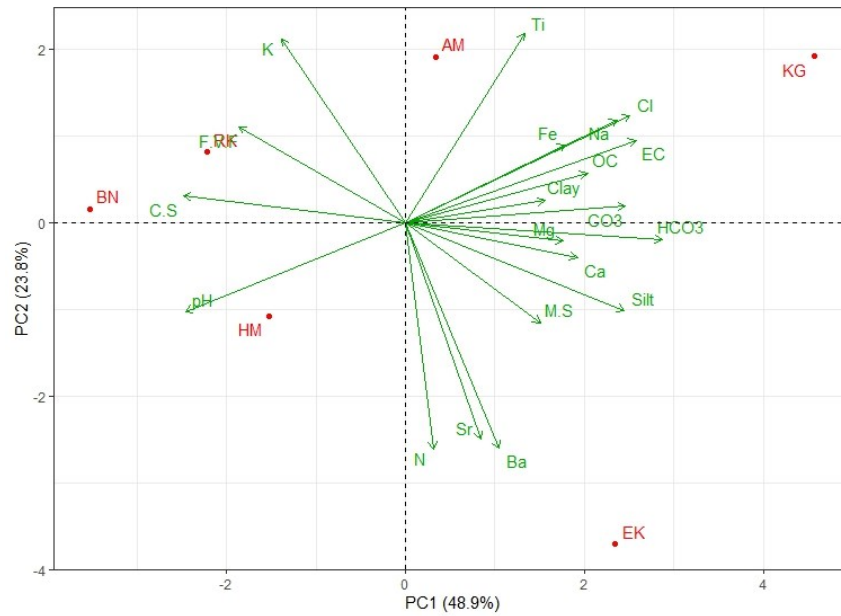
284
 285 **Figure 6.** Cluster Heat Map for the relationship between the sites, heavy metals, nutrients and
 286 sediment grain sizes.

287 3.8 Principal Component Analysis

288 The principal component analysis (PCA) biplot and contribution plot (figure 7) for the influence
 289 of sediment grain sizes on heavy metals, nutrients and soil properties in the different sites revealed
 290 a total variation of 72.7 % contributed by PC1 48.9% and PC2 by 23.8% respectively. Based on
 291 the aforementioned total variation by the PCs, a positive correlation exists between clay grain types
 292 and Fe, Na, Ti, Cl, OC, EC and CO₃, influenced by site AM and KG (figure 6). Additionally, the
 293 silt grain type was positively correlated with Mg, HCO₃, Ca, M.S, Ba, Sr, and N, and was
 294 influenced by site EK. It is important to note that overall in terms of contribution to relationships
 295 revealed by the PCA, Clay and Mg had the lowest contribution (figure 8).

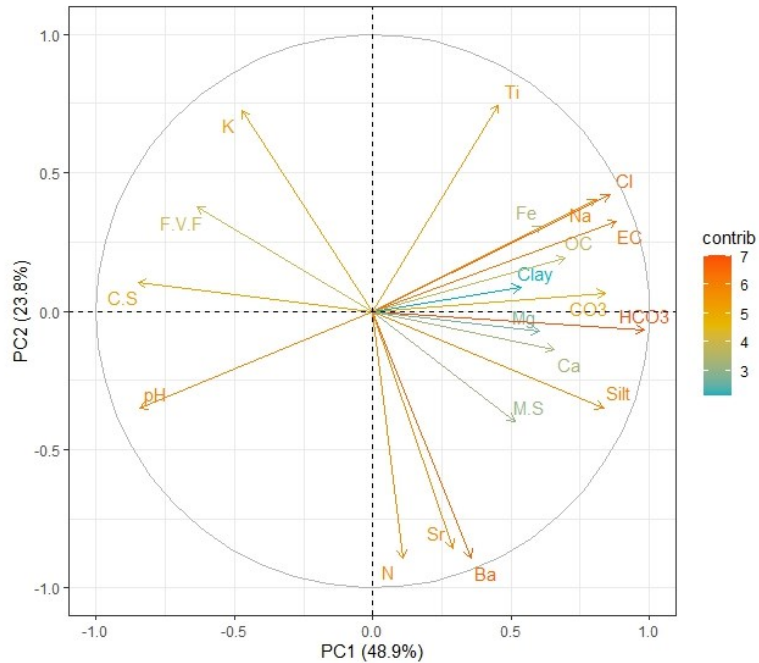
296

297



299

300 **Figure 7.** Principal Component Analysis (PCA) biplot for the influence of sediment grain sizes on
 301 heavy metals, nutrients and sediment properties .



302

303 **Figure 8.** Principal Component Analysis contribution plot for the influence of sediment grain sizes
 304 on heavy metals, nutrients and sediment properties.

305

306

307 **4. Discussion**

308 The current data investigates the accumulation of trace elements Ca and Fe and heavy metals in
309 mangrove species *A. marina* leaves and examines the OC, N, Mg, and Ca contents of sediment
310 particles at six red sea coastal areas. To survive in their extreme environment, mangrove plants
311 have developed a number of specific adaptations, such as diverse root systems and altered bark
312 and leaf structures. The present research showed higher Ca and Fe were noted in the southern
313 locations of the Red Sea coast, by 35.9 mg/kg and 31.6 mg/kg in the RK and BN, respectively.
314 Mangrove positions in the north and south Red Sea are considered to have low leaf nutrient
315 concentrations, mostly Ca and Fe, indicating the possibility of nutrient limitation in north and south
316 Red Sea mangroves throughout the stands. The mangrove species *Avicennia* species are considered
317 to have better resistance tolerance and acquire several compared to other mangrove species (Parida
318 and Jha, 2010; Wang et al., 2022). Therefore, Ca and Fe are important nutrients for limiting plant
319 growth, where nitrogen increases the number of leaves in plants. Fe mostly to enhanced root
320 development. This crucial micronutrient, Fe, and its uptake and distribution to plant parts are
321 necessary for the photosynthetic process and leaf tissue (Solangi et al., 2023). A previous study
322 found that five mangrove species living in north Queensland, Australia, had significant iron
323 requirements from the seedling to tree stage of development (Almahasheer H, 2006).
324 Furthermore, the high concentration of these nutrients in mangrove leaves may be that these metals
325 are micronutrients that are essential metals for mangrove growth and metabolism and thus are
326 absorbed and used by mangrove plants. Fe is toxic when high levels accumulate; it could act with
327 catalytic by Fenton reaction to generate hydroxyl radicals, which could damage lipids, proteins,
328 and DNA. However, the current study showed that Sr concentration is higher in mangrove leaves
329 than Ba and Ti in the EK north region of the Red Sea (table 1).

330 The previous study demonstrated similar results: strontium was easily transferred to the
331 aboveground part of soybean (Dresler et al., 2018). In its stable forms, strontium is not particularly
332 toxic to plants. However, it frequently has a negative impact on the uptake of specific nutrients,
333 mostly calcium, due to its negative impact on plant development and growth (Burger and
334 Lichtscheidl, 2019). It is noted that strontium was quickly transferred to the leaves, and in general,
335 its accumulation in plant parts was reduced as follows: leaves > stems > roots > seeds. Different
336 types of mangrove species and the various ranges of heavy metal concentrations would affect the

337 bioavailability of the heavy metal potential of mangroves and their environment (Dubey et al.,
338 2018).

339 The current study results showed the soil EC range fluctuates between the highest 6.5 EC (dS/m)
340 and the lowest 2.2, while soil pH was slightly alkaline throughout the north and south regions of
341 the study area. This may impact the mangrove species found in the different types of mangrove
342 ecosystems due to the salinity levels that fluctuate due to high temperatures and oceanic
343 fluctuations (Barik et al., 2018). The salinity could have been described by different particle sizes
344 and mineral compositions in soil sediment (Fernandes et al., 2019). However, the carbonate-
345 bearing (calcite and aragonite) and evaporated (halite) minerals are widely famous for salinity
346 control (F. Solangi et al., 2019). It is noted by previous studies(Alsamadany et al., 2020; Usman et
347 al., 2013), that most of the pH levels, which were shown by some researchers in sediment samples
348 of coastal areas, were alkaline and fluctuated between 7.49 and 8.51 in their study at sites 6 and
349 13, respectively. The distribution of particle sizes in sediments is often considered an effective tool
350 for investigating the tectonic pathways and their parent material origin. The percentages of the
351 size of sediment particles and their distribution present results were found the fine sand and very
352 fine sand particles (range between 26% to 34%) were dominant across the various location and
353 highest percentages of fine sand particles was found in south regions (Fig 4). Similar results were
354 observed in an earlier study: sediment particles formed of sand varied between 64.10 and 94.60%,
355 while the fine mud fraction was 5.40%. The presence of fine sediment particles in mostly all the
356 sediment samples is possibly due to many reasons, including the parent material, urban intrusion,
357 and degradation of coastlines along the experimental area. Changes in sediment deposition
358 patterns, particularly for fine particles, and chemical processes can be attributed for the different
359 distributions of heavy metals in sediments across large regional scales (Naz et al., 2023).

360 The difference in sediment grain size in the oceans can be influenced by a variety of factors,
361 including sedimentary behavior and sediment transportation. Multiple studies have demonstrated
362 that mangrove ecosystems can enhance the amount of suspended solids formed by decreasing
363 water dynamics and allowing fine-grained sediments, which are a primary source of minor element
364 absorbance, to have more time to deposit (Talukdar et al., 2023; Xiong et al., 2018). The present
365 study showed salt such as Na^+ , Cl^- , HCO_3^- and CO_3^{2-} were significantly affected by the coastline
366 Red Sea area. Na and Cl are important micronutrients in plants and participate in various
367 physicochemical processes (Colmenero-Flores et al., 2019; Raven, 2017). The Seawater alkaline

368 nature is simplified as the charge balance of conservative ions (Na^+ , Ca^{2+} , K^+ , Cl^-) and some
369 minor elements' redox state (Krumins et al. 2013). The primary sources of the HCO_3^- concentration
370 were organic and terrigenous elements obtained from the soil. It has been shown to be crucial in
371 regulating the potentially hazardous elements (Mosa et al., 2016). However, the mean value
372 percentages of soil OC, soil N, Mg, and Ca (soluble salts) varies between locations in the north
373 and south of the Red Sea coastline. Worldwide red sea area covered with mangrove ecosystems
374 have been reported lowest OC ranges by $15 \text{ g m}^{-2} \text{ yr}^{-1}$ which is many times lower than the average
375 global estimate of $163 \text{ g m}^{-2} \text{ yr}^{-1}$ of OC. The nutrient cycling nitrogen and phosphorus is a key
376 factor influencing the seawater inorganic carbon system and the global carbon cycle (Dai et al.,
377 2018). Nitrogen is a major element for plant growth, and Mg is an alkaline micronutrient in ionic
378 form by plants (Solangi et al., 2023). The Mg ions are involved in chlorophyll-related processes
379 within the plant and are moderately more present in seawater than the other major elements
380 (Saderne et al., 2018). A wide range of interacting influences between several critical nutrients and
381 the calcium-rich soils on Aldabra is likely to occur (Solangi et al., 2024). It promotes the
382 application of a composite variable to describe the complete effect of nutrient content on
383 mangroves.

384 The association revealed by the cluster heat map with the independent variables forming two
385 groups, comprising a group with Na, Cl, F+V.F, clay, silt, OC, and M.S, indicates that Na, Cl, OC,
386 and M.S are more related to finer grain types like clay and silt. However, the grouping of Sr, Mg,
387 Ti, EC, Fe, CO_3 , K, C.S, HCO_3^- , Ca, pH, and N in the second group suggests a distinct cluster and
388 implies a specific geochemical and granulometric association, helping to understand nutrient and
389 contaminant distribution (Unda-Calvo et al., 2019). Our findings align with the previous study
390 (Toller et al., 2021) except for KG's unique Na and Cl association, indicating localized influences.
391 The positive correlation between clay grain types and Fe, Na, Ti, Cl, OC, EC, and CO_3 , with sites
392 AM and KG influencing these variables, and the positive correlation between silt grain type with
393 Mg, HCO_3^- , Ca, M.S, Ba, Sr, and N, influenced by site EK, with low contributions of clay and Mg
394 suggests that while they are present, their impact is minimal compared to other factors (Sing,
395 2022). These results align with a previous study (Moquet et al., 2021), except for the unique
396 correlations between AM and KG sites, indicating site-specific influences.

397 5. Conclusion

398 This study investigates the *A. marina* mangrove species, leaves sequester a substantial amount of
399 Ca and Fe in the Red Sea. The Ca higher range in mangrove leaves was observed at two south
400 locations of the Red Sea coast, by RK and BN, at 35.9 mg/kg and 31.6 mg/kg. In this research,
401 heavy metal concentration in mangrove leaves does not reflect the comprehensive picture of heavy
402 metal status in mangroves and its temporal appropriation of these metals. Meanwhile, the Na⁺,
403 Cl⁻, HCO₃⁻, and CO₃²⁻ were recorded in the northern region of the Red Sea coastline. Fine and
404 very fine sand particles were dominant, mostly in the BN sites, with 34.7% in the south area of the
405 study region. However, the percentages of organic carbon (OC), calcium (Ca), magnesium (Mg),
406 and nitrogen (N) were found in the north region of the studied side. Further study need to clarify
407 the heavy metal concentration of mangroves roots and plant total biomass nutrient content. Other
408 toxic heavy metal concentrations further investigate the soil sediments in the Red Sea area in
409 Sudan.

410 **CRedit authorship contribution statement**

411 **Rabha K M Khalil:** Investigation, Formal analysis, Data curation. **Kashif A Solangi:** review & editing,
412 Writing – original draft, Formal analysis. **Abdullahi B Alhassan:** Formal analysis, Writing – review &
413 editing. **Waseem R Khan:** review & editing and **Mohammed O Aljahdali** Supervision, Project
414 administration, Funding acquisition, Conceptualization

415 **Declaration of competing interest**

416 The authors declare that they have no known competing financial interests or personal
417 relationships that could have appeared to influence the work reported in this paper.

418 **Acknowledgments**

419 The authors would like to acknowledge that this research was funded entirely through personal resources.
420 No external grants or financial support were received for this study.

421 **Data availability**

422 Data will be made available on request.

423 **References**

- 424 Abou Seedo, K., Abido, M.S., Salih, A.A., Abahussain, A., 2017. Assessing heavy metals
425 accumulation in the leaves and sediments of urban mangroves (*Avicennia marina* (Forsk.)
426 Vierh.) in Bahrain. *Int. J. Ecol.* 2017.
427 Afzaal, M., Hameed, S., Liaqat, I., Ali Khan, A.A., Abdul Manan, H., Shahid, R., Altaf, M.,

428 2022. Heavy metals contamination in water, sediments and fish of freshwater ecosystems in
429 Pakistan. *Water Pract. Technol.* 17, 1253–1272.

430 Ahmed, H.E.H., 2014. Determination of trace elements in plant samples using XRF, PIXE and
431 ICP-OES techniques.

432 Ali Solangi, K., Wu, Y., Xing, D., Ahmed Qureshi, W., Hussain Tunio, M., Ali Sheikh, S.,
433 Shabbir, A., 2022. Can electrophysiological information reflect the response of mangrove
434 species to salt stress? A case study of rewatering and Sodium nitroprusside application.
435 *Plant Signal. Behav.* 17. <https://doi.org/10.1080/15592324.2022.2073420>

436 Aljahdali, M.O., Alhassan, A.B., 2020. Ecological risk assessment of heavy metal contamination
437 in mangrove habitats, using biochemical markers and pollution indices: A case study of
438 *Avicennia marina* L. in the Rabigh lagoon, Red Sea. *Saudi J. Biol. Sci.* 27, 1174–1184.

439 Alsamadany, H., Al-Zahrani, H.S., Selim, E.-M.M., El-Sherbiny, M.M., 2020. Spatial
440 distribution and potential ecological risk assessment of some trace elements in sediments
441 and grey mangrove (*Avicennia marina*) along the Arabian Gulf coast, Saudi Arabia. *Open*
442 *Chem.* 18, 77–96.

443 Anu, K., Sneha, V.K., Busheera, P., Muhammed, J., Augustine, A., 2024. Mangroves in
444 environmental engineering: Harnessing the multifunctional potential of Nature’s coastal
445 architects for sustainable ecosystem management. *Results Eng.* 101765.

446 Arumugam, G., Rajendran, R., Ganesan, A., Sethu, R., 2018. Bioaccumulation and translocation
447 of heavy metals in mangrove rhizosphere sediments to tissues of *Avicennia marina*—A field
448 study from tropical mangrove forest. *Environ. nanotechnology, Monit. Manag.* 10, 272–
449 279.

450 Ashournejad, Q., Amiraslani, F., Moghadam, M.K., Toomanian, A., 2019. Assessing the changes
451 of mangrove ecosystem services value in the Pars Special Economic Energy Zone. *Ocean*
452 *Coast. Manag.* 179, 104838.

453 Aslam, R.W., Shu, H., Naz, I., Quddoos, A., Yaseen, A., Gulshad, K., Alarifi, S.S., 2024a.
454 Machine Learning-Based Wetland Vulnerability Assessment in the Sindh Province Ramsar
455 Site Using Remote Sensing Data. *Remote Sens.* 16, 928.

456 Aslam, R.W., Shu, H., Tariq, A., Naz, I., Ahmad, M.N., Quddoos, A., Javid, K., Mustafa, F.,
457 Aeman, H., 2024b. Monitoring landuse change in Uchhali and Khabeki wetland lakes,
458 Pakistan using remote sensing data. *Gondwana Res.* 129, 252–267.

459 Aslam, R.W., Shu, H., Yaseen, A., Sajjad, A., Abidin, S.Z.U., 2023. Identification of time-
460 varying wetlands neglected in Pakistan through remote sensing techniques. *Environ. Sci.*
461 *Pollut. Res.* 30, 74031–74044.

462 Badarudeen, A., Sajan, K., Srinivas, R., Maya, K., Padmalal, D., 2014. Environmental
463 significance of heavy metals in leaves and stems of Kerala mangroves, SW coast of India.

464 Barik, J., Mukhopadhyay, A., Ghosh, T., Mukhopadhyay, S.K., Chowdhury, S.M., Hazra, S.,
465 2018. Mangrove species distribution and water salinity: an indicator species approach to
466 Sundarban. *J. Coast. Conserv.* 22, 361–368. <https://doi.org/10.1007/s11852-017-0584-7>

467 Bartolini, F., Cimò, F., Fusi, M., Dahdouh-Guebas, F., Lopes, G.P., Cannicci, S., 2011. The
468 effect of sewage discharge on the ecosystem engineering activities of two East African
469 fiddler crab species: consequences for mangrove ecosystem functioning. *Mar. Environ. Res.*
470 71, 53–61.

471 Burger, A., Lichtscheidl, I., 2019. Strontium in the environment: Review about reactions of
472 plants towards stable and radioactive strontium isotopes. *Sci. Total Environ.* 653, 1458–
473 1512.

474 Chen, K., Chen, L., Fan, J., Fu, J., 2013. Alleviation of heat damage to photosystem II by nitric
475 oxide in tall fescue. *Photosynth. Res.* 116, 21–31. [https://doi.org/10.1007/s11120-013-9883-](https://doi.org/10.1007/s11120-013-9883-5)
476 5

477 Clapera, R.S., 2006. Energy dispersive X-ray fluorescence: Measuring elements in solid and
478 liquid matrices.

479 Colmenero-Flores, J.M., Franco-Navarro, J.D., Cubero-Font, P., Peinado-Torrubia, P., Rosales,
480 M.A., 2019. Chloride as a beneficial macronutrient in higher plants: new roles and
481 regulation. *Int. J. Mol. Sci.* 20, 4686.

482 Dai, Z., Trettin, C.C., Frolking, S., Birdsey, R.A., 2018. Mangrove carbon assessment tool:
483 Model development and sensitivity analysis. *Estuar. Coast. Shelf Sci.* 208, 23–35.

484 Dasgupta, S., 2007. The impact of sea level rise on developing countries: a comparative analysis.
485 World Bank Publications.

486 Dresler, S., Wójciak-Kosior, M., Sowa, I., Strzemiński, M., Sawicki, J., Kováčik, J., Blicharski, T.,
487 2018. Effect of long-term strontium exposure on the content of phytoestrogens and allantoin
488 in soybean. *Int. J. Mol. Sci.* 19, 3864.

489 Dubey, S., Shri, M., Gupta, A., Rani, V., Chakrabarty, D., 2018. Toxicity and detoxification of

490 heavy metals during plant growth and metabolism. *Environ. Chem. Lett.* 16, 1169–1192.

491 Dudani, S.N., Lakhmapurkar, J., Gavali, D., Patel, T., 2017. Heavy metal accumulation in the
492 mangrove ecosystem of south Gujarat coast, India. *Turkish J. Fish. Aquat. Sci.* 17, 755–766.

493 Ebrahim, A.M., Eltayeb, M.H., Khalid, H., Mohamed, H., Abdalla, W., Grill, P., Michalke, B.,
494 2012. Study on selected trace elements and heavy metals in some popular medicinal plants
495 from Sudan. *J. Nat. Med.* 66, 671–679.

496 Einollahipeer, F., Khammar, S., Sabaghzadeh, A., 2013. A study on heavy metal concentration in
497 sediment and mangrove (*Avicenia marina*) tissues in Qeshm island, Persian Gulf. *J. Nov.*
498 *Appl. Sci.* 2, 498–504.

499 Fernandes, E., Vitorino, N., Ribeiro, M.J., Teixeira, C., Bordalo, A.A., 2019. Spatial and
500 seasonal dynamics of elemental composition and mineralogy of intertidal and subtidal
501 sediments in the Lima estuary (NW Portugal). *Arab. J. Geosci.* 12, 1–13.

502 Jimenez, L.C.Z., Queiroz, H.M., Otero, X.L., Nóbrega, G.N., Ferreira, T.O., 2021. Soil organic
503 matter responses to Mangrove restoration: A replanting experience in Northeast Brazil. *Int.*
504 *J. Environ. Res. Public Health* 18, 8981.

505 Kamaruzzaman, B.Y., Ong, M.C., Jalal, K.C.A., Shahbudin, S., Nor, O.M., 2009. Accumulation
506 of lead and copper in *Rhizophora apiculata* from Setiu mangrove forest, Terengganu,
507 Malaysia. *J. Environ. Biol.* 30, 821.

508 Khan, W.R., Aljahdali, M.O., 2022. Elemental composition of above and belowground
509 mangrove tissue and sediment in managed and unmanaged compartments of the Matang
510 Mangrove Forest Reserve. *Plants* 11, 2916.

511 Mosa, A., El-Ghamry, A., Trüby, P., Omar, M., Gao, B., Elnaggar, A., Li, Y., 2016. Chemo-
512 mechanical modification of cottonwood for Pb²⁺ removal from aqueous solutions: Sorption
513 mechanisms and potential application as biofilter in drip-irrigation. *Chemosphere* 161, 1–9.

514 Naz, I., Ahmad, I., Aslam, R.W., Quddoos, A., Yaseen, A., 2023. Integrated assessment and
515 geostatistical evaluation of groundwater quality through water quality indices. *Water* 16, 63.

516 Nazli, M.F., Hashim, N.R., 2010. Heavy metal concentrations in an important mangrove species,
517 *Sonneratia caseolaris*, in Peninsular Malaysia. *Environ. Asia* 3, 50–55.

518 Nguyen, A., Richter, O., Le, B.V.Q., Phuong, N.T.K., Dinh, K.C., 2020. Long-term heavy metal
519 retention by mangroves and effect on its growth: A field inventory and scenario simulation.
520 *Int. J. Environ. Res. Public Health* 17, 9131.

521 Parida, A.K., Jha, B., 2010. Salt tolerance mechanisms in mangroves: A review. *Trees - Struct.*
522 *Funct.* 24, 199–217. <https://doi.org/10.1007/s00468-010-0417-x>

523 Raven, J.A., 2017. Chloride: essential micronutrient and multifunctional beneficial ion. *J. Exp.*
524 *Bot.* 68, 359–367.

525 Roumié, M., Nsouli, B., Zahraman, K., Reslan, A., 2004. First accelerator based ion beam
526 analysis facility in Lebanon: development and applications. *Nucl. Instruments Methods*
527 *Phys. Res. Sect. B Beam Interact. with Mater. Atoms* 219, 389–393.

528 Saderne, V., Cusack, M., Almahasheer, H., Serrano, O., Masqué, P., Arias-Ortiz, A.,
529 Krishnakumar, P.K., Rabaoui, L., Qurban, M.A., Duarte, C.M., 2018. Accumulation of
530 carbonates contributes to coastal vegetated ecosystems keeping pace with sea level rise in
531 an arid region (Arabian Peninsula). *J. Geophys. Res. Biogeosciences* 123, 1498–1510.

532 Saoum, M.R., Sarkar, S.K., 2024. Monitoring mangrove forest change and its impacts on the
533 environment. *Ecol. Indic.* 159, 111666. <https://doi.org/10.1016/j.ecolind.2024.111666>

534 Solangi, F., Bai, J., Gao, S., Yang, L., Zhou, G., Cao, W., 2019. Improved accumulation
535 capabilities of phosphorus and potassium in green manures and its relationship with soil
536 properties and enzymatic activities. *Agronomy* 9. <https://doi.org/10.3390/agronomy9110708>

537 Solangi, F., Zhu, X., Khan, S., Rais, N., Majeed, A., Sabir, M.A., Iqbal, R., Ali, S., Hafeez, A.,
538 Ali, B., 2023. The Global Dilemma of Soil Legacy Phosphorus and Its Improvement
539 Strategies under Recent Changes in Agro-Ecosystem Sustainability. *ACS omega* 8, 23271–
540 23282.

541 Solangi, K.A., Abbasi, B., Solangi, F., Khaskhali, S., Siyal, A.A., Mehmood, H., Irfan, M., 2024.
542 Assessment of Saturated Hydraulic Conductivity with Using Soil Particle Size Distribution:
543 A Comparative Study of Constant Head and Falling Head Methods. *Glob. NEST J.* 26, 1–9.
544 <https://doi.org/10.30955/gnj.005833>

545 Solangi, K.A., Siyal, A.A., Wu, Y., Abbasi, B., Solangi, F., Lakhari, I.A., Zhou, G., 2019. An
546 assessment of the spatial and temporal distribution of soil salinity in combination with field
547 and satellite data: A case study in Sujawal district. *Agronomy* 9.
548 <https://doi.org/10.3390/agronomy9120869>

549 Solangi, K.A., Wu, Y., Chen, Q., Qureshi, W.A., Xing, D., Tunio, M.H., Shaikh, S.A., 2021. The
550 differential responses of *Aegiceras corniculatum* and *Kandelia candel* under salt stress and
551 re-watering phase . A study of leaf electrophysiological and growth parameters.

552 <https://doi.org/10.1080/17429145.2021.1946606>

553 Talukdar, A., Kundu, P., Bhattacharjee, S., Dey, S., Dey, A., Biswas, J.K., Chaudhuri, P.,
554 Bhattacharya, S., 2023. Microplastics in mangroves with special reference to Asia:
555 Occurrence, distribution, bioaccumulation and remediation options. *Sci. Total Environ.*
556 166165.

557 Usman, A.R.A., Alkredaa, R.S., Al-Wabel, M.I., 2013. Heavy metal contamination in sediments
558 and mangroves from the coast of Red Sea: *Avicennia marina* as potential metal
559 bioaccumulator. *Ecotoxicol. Environ. Saf.* 97, 263–270.

560 Wang, N., Naz, I., Aslam, R.W., Quddoos, A., Soufan, W., Raza, D., Ishaq, T., Ahmed, B., 2024.
561 Spatio-Temporal Dynamics of Rangeland Transformation using machine learning
562 algorithms and Remote Sensing data. *Rangel. Ecol. Manag.* 94, 106–118.

563 Wang, S.M., Wang, Y.S., Su, B.Y., Zhou, Y.Y., Chang, L.F., Ma, X.Y., Li, X.M., 2022.
564 Ecophysiological Responses of Five Mangrove Species (*Bruguiera gymnorrhiza*,
565 *Rhizophora stylosa*, *Aegiceras corniculatum*, *Avicennia marina*, and *Kandelia obovata*) to
566 Chilling Stress. *Front. Mar. Sci.* 9, 1–8. <https://doi.org/10.3389/fmars.2022.846566>

567 Xiong, Y., Liao, B., Wang, F., 2018. Mangrove vegetation enhances soil carbon storage
568 primarily through in situ inputs rather than increasing allochthonous sediments. *Mar. Pollut.*
569 *Bull.* 131, 378–385.

570